Supporting information

Electrochemically activated Co-Prussian blue analogue derived amorphous CoB nanostructures: Efficient electrocatalyst for oxygen evolution reaction

Rajat K. Tripathy,[a, b, c] Aneeya K. Samantara [a, b, c] and J. N Behera [a, b, c*]

[a] School of Chemical Sciences, National Institute of Science Education and Research (NISER), P. O. Jatni, Khurda 752050, Odisha, India.

[b] Homi Bhabha National Institute (HBNI), Mumbai, India.

[c] Centre for Interdisciplinary Sciences (CIS), NISER, Jatni, Odisha, India 752050.

E-mail: jnbehera@niser.ac.in

Composition and structure of Co-PBA:

The Cobalt Prussian blue analogue (Co PBA, $Co_3[Co(CN)_6])_2 \cdot xH_2O$) belongs to face centred cubic phase with space group $Fm\bar{3}m$ contains Co^{+2} and Co^{+3} ion. Cyanide groups are connected to both type of cobalt ion in different fashion mode. The outer Co^{+2} ion attached to six nitrogen atom of cyanide ligand whereas inner Co^{+3} ion coordinated to six carbon atom of cyanide ligand forming a framework with large voids. These voids are occupied by water molecules in different modes s.a present in interstitial site or coordinated to deficiency bonded metal ions or water which is hydrogen bonded coordinated to water molecule.[1,2]

Electrochemical calculations:

The intrinsic electrocatalytic activity of all the electrocatalysts were determined by iR compensating the recorded polarization plots as per the following equation,

$$E_{iR\ corrected} = E_{observed} - iR \quad \ldots\ldots\ldots\ldots\ldots\ldots\ldots\ldots\ldots\ldots\ldots\ldots\ldots.. (1)$$

Here, I and R are the observed anodic current and solution resistance (R_s) of the electrocatalyst. The Rs was obtained from the Nyquist impedance spectrum recorded in the frequency range of 1 MHz to 0.1 Hz at an applied amplitude of 5 mV.

After calculation of the electrochemical active surface area, the roughness factor was calculated by normalizing the ECSA with the geometrical surface area of the glassy carbon electrode. The turnover frequency (TOF) of the CoB@300, CoB@450, CoB@550 and CoB@650 was calculated by assuming the participation of all the metal atoms in the electrocatalysis process as per the following equation, [3,4]

$$TOF = \frac{J \times S}{4Fn} \quad \ldots\ldots\ldots\ldots\ldots\ldots\ldots\ldots\ldots\ldots\ldots\ldots\ldots.. (2)$$

Here, J, S, F and n are the observed OER current density, geometrical surface area of the glassy carbon electrode, Faraday constant (96485.3 C/mol) and moles of catalytically active sites respectively. The value of "n" was calculated by dividing the mass of the electrocatalyst casted on the electrode surface by molecular mass. Since one molecule of oxygen evolved along with four number of electrons, so the term 4 is taken in the denominator.
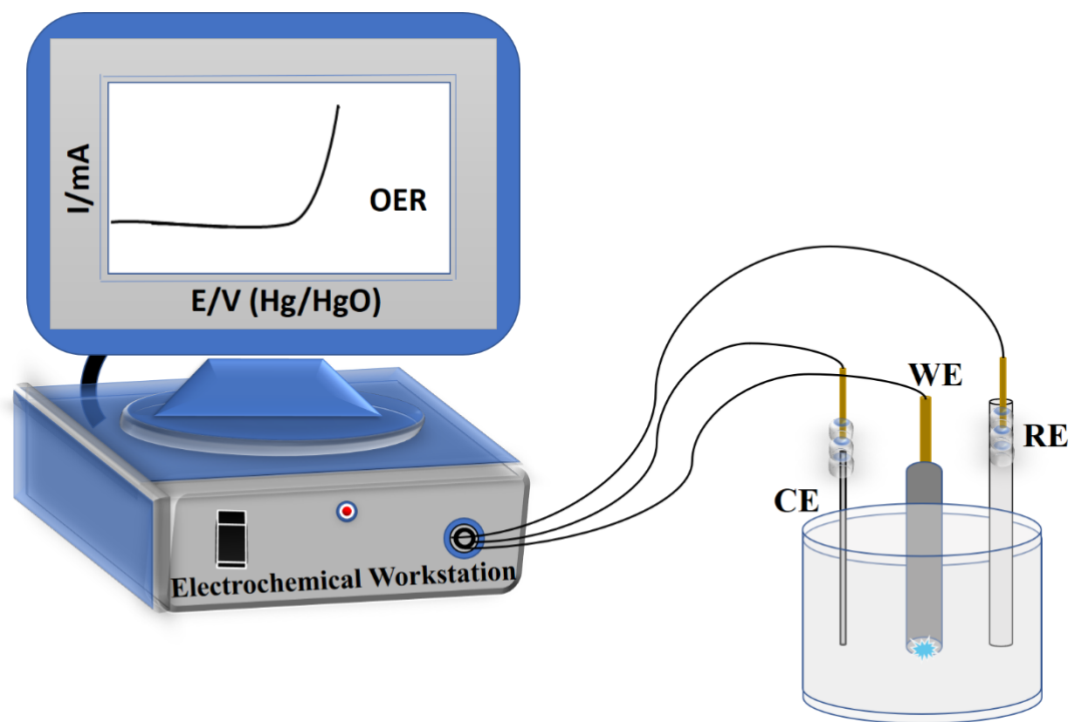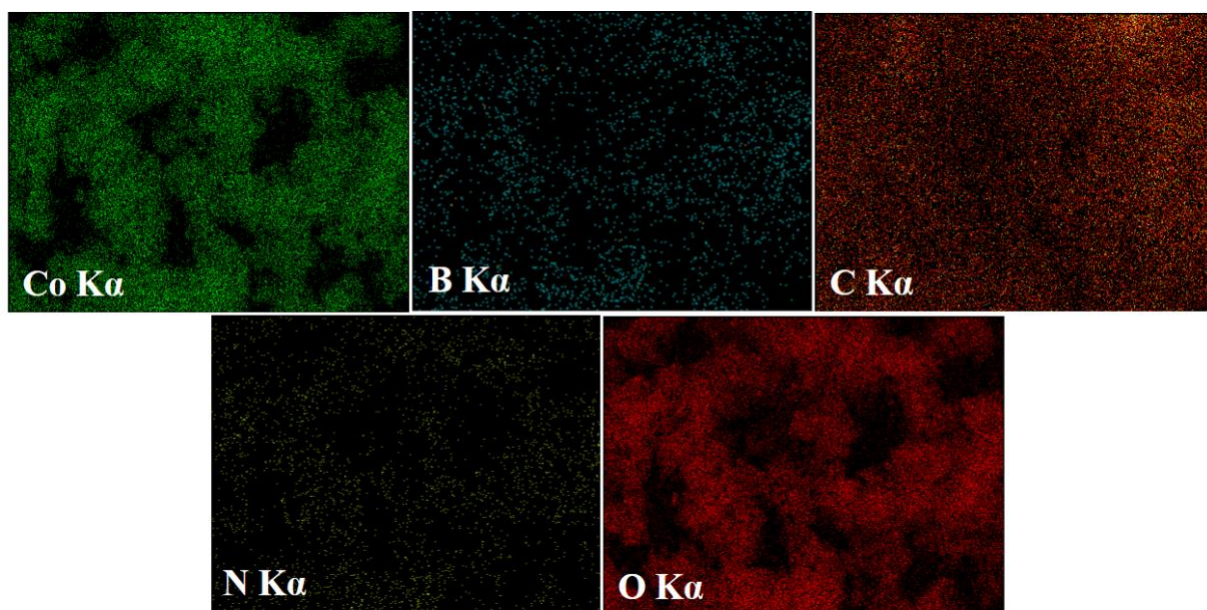
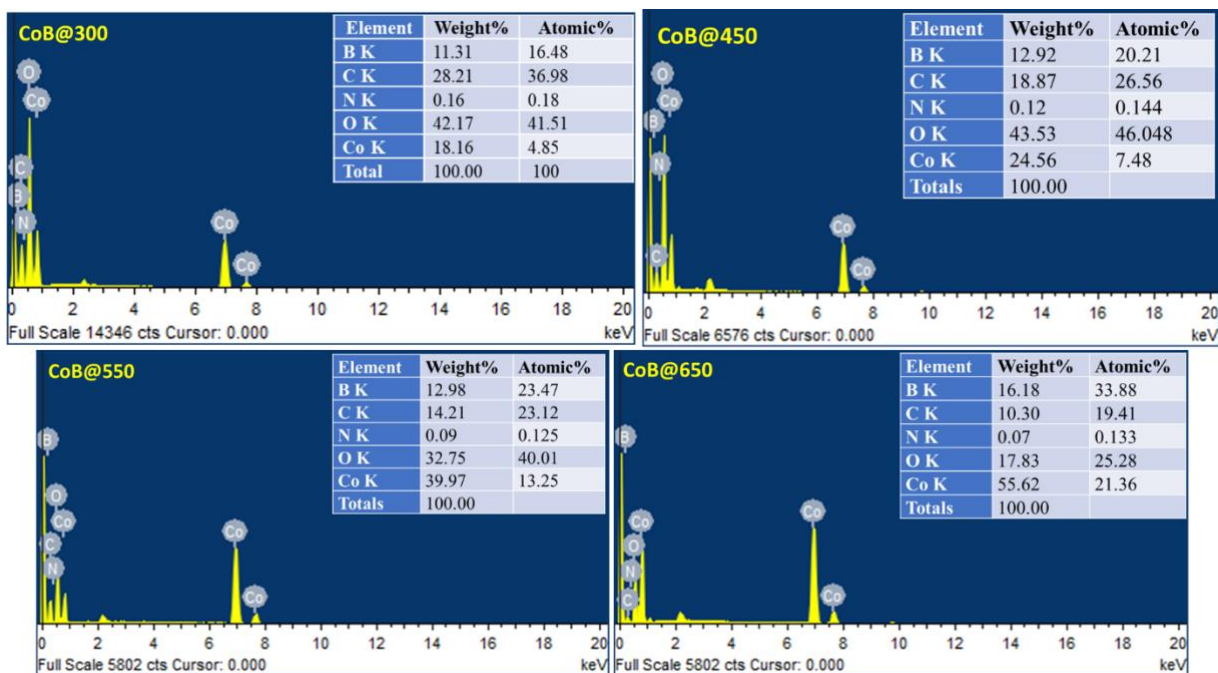**Fig. S 1** Schematic presentation of three electrode electrochemical cell
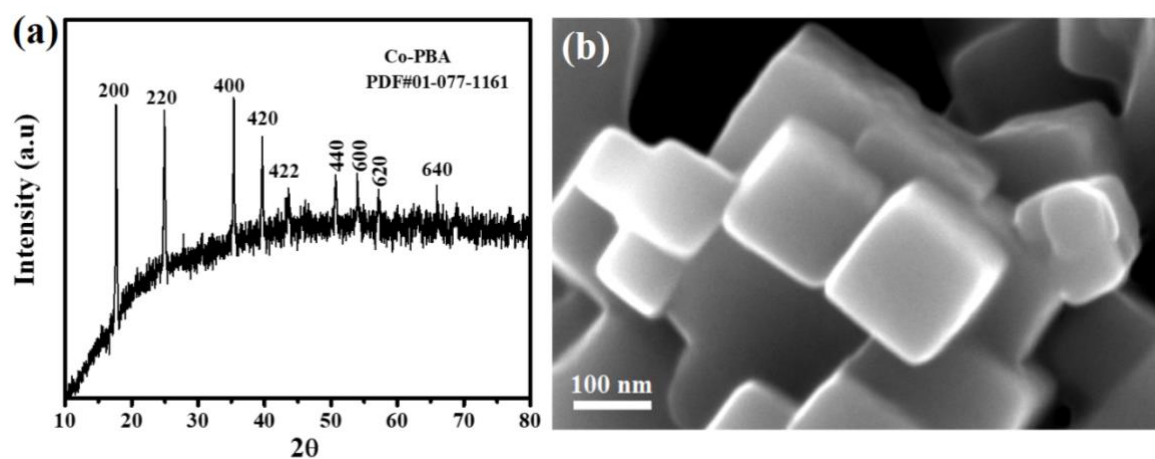
Fig. S 2 (a) X-ray diffraction pattern and (b) FESEM for the Co-PBA.
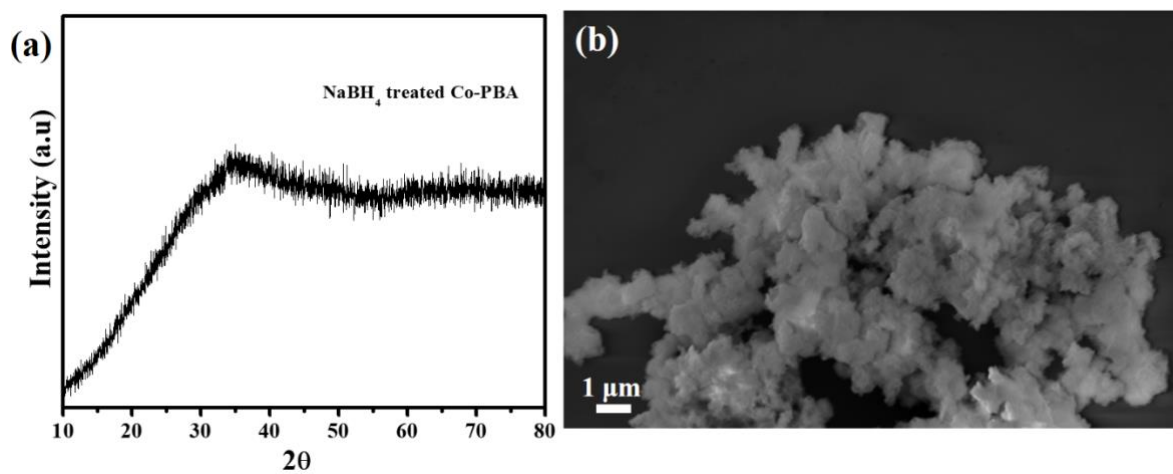
**Fig. S 3** (a) X-ray diffraction pattern and (b) FESEM image of Co-PBA after treating with NaBH4.

Fig. S 4 Elemental mapping for CoB@300.

Fig. S 5 The EDS showing the presence of different elements in CoB annealed at different temperatures and the inset shows the corresponding weight and atomic percentage of elements.

Sample name	Carbon	Hydrogen	Nitrogen
CoB@300	1.312	2.102	0.28
CoB@450	1.116	1.905	0.051
CoB@550	0.738	0.639	0.064
CoB@650	0.604	0.608	0.048

Table S 1 CHN analysis report of CoB@300, CoB@450, CoB@550 and CoB@650.
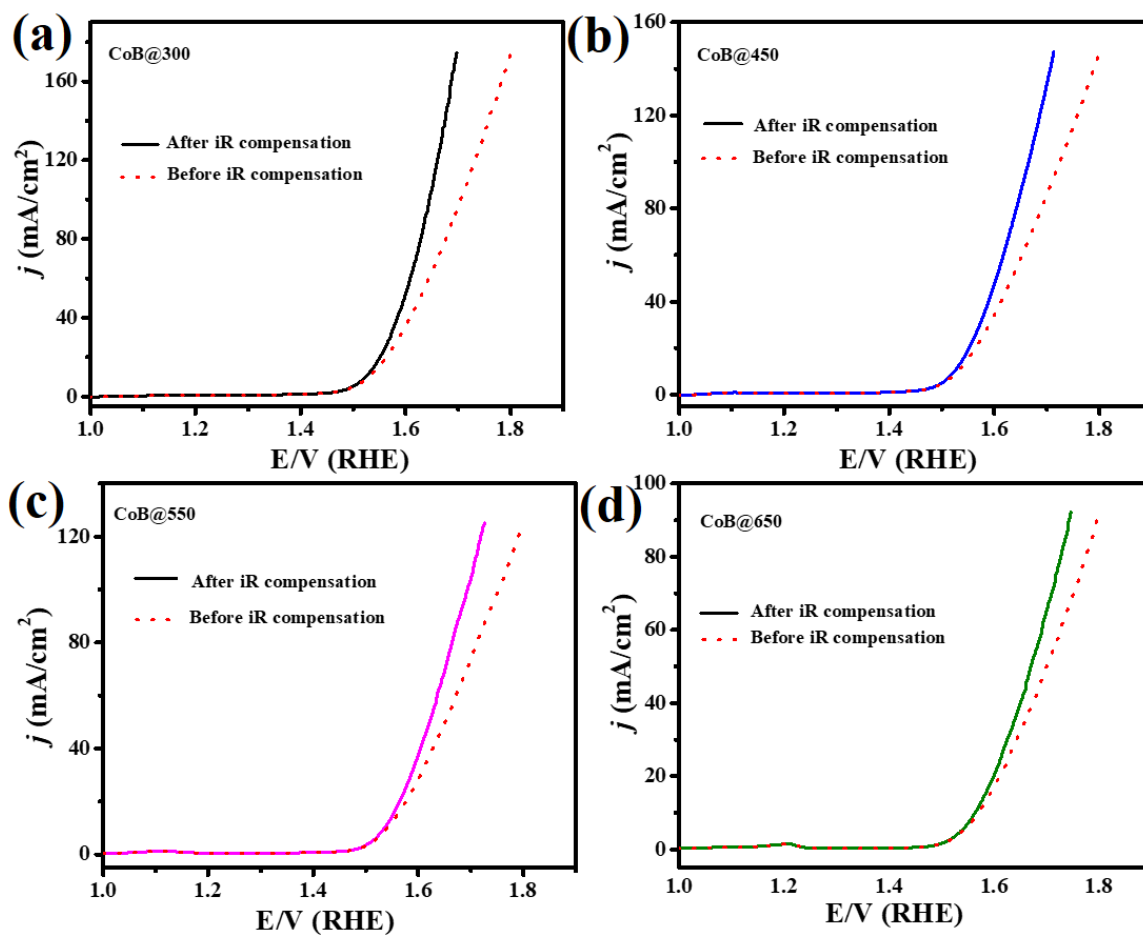
Fig. S 6 Linear sweep voltammograms for the (a) CoB@300, (b) CoB@450, (c) CoB@550 and (d) CoB@650 before and after iR-compensation.
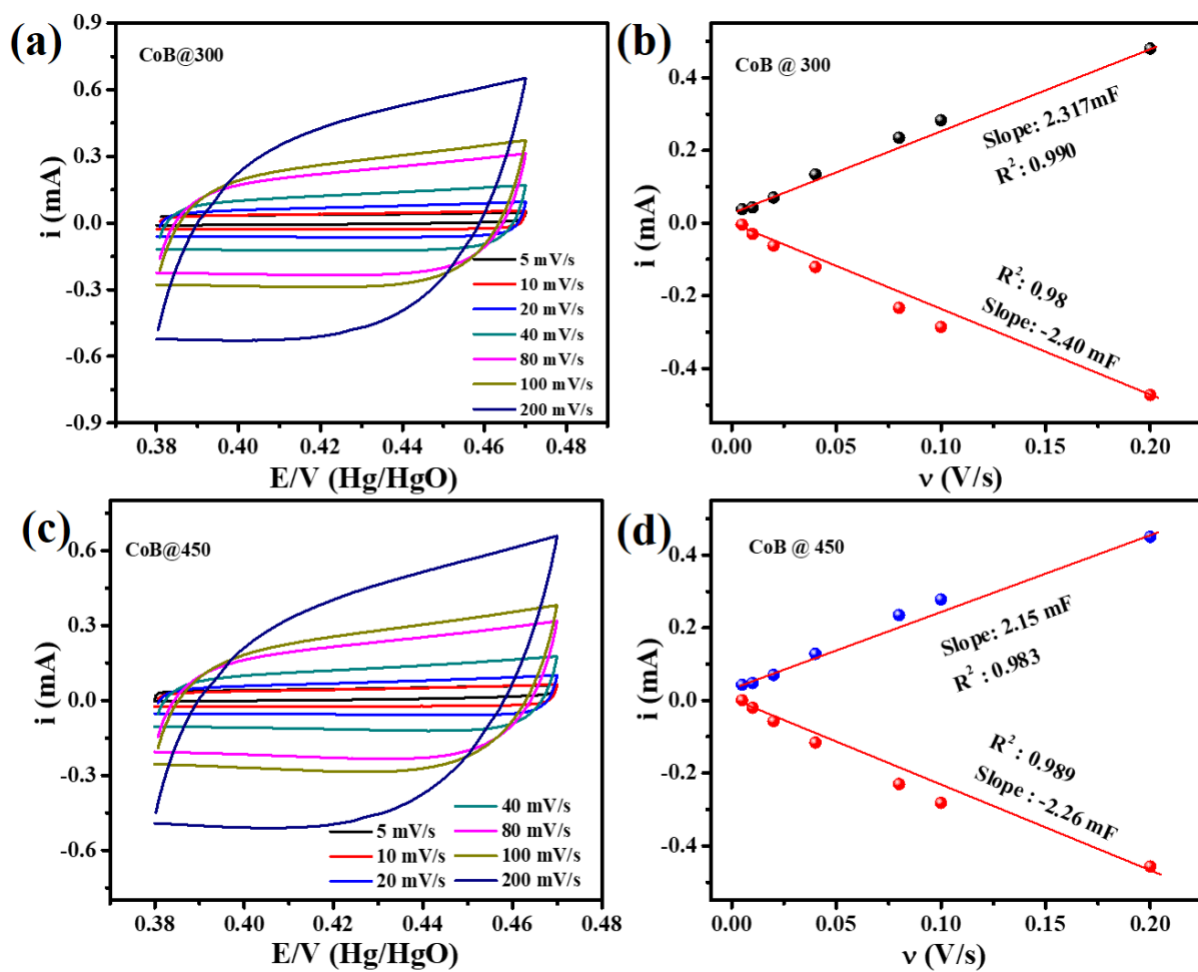
Fig. S 7 (a, c) Cyclic voltammograms and (b, d) plot of current at different sweep rate for CoB@300 and CoB@450.
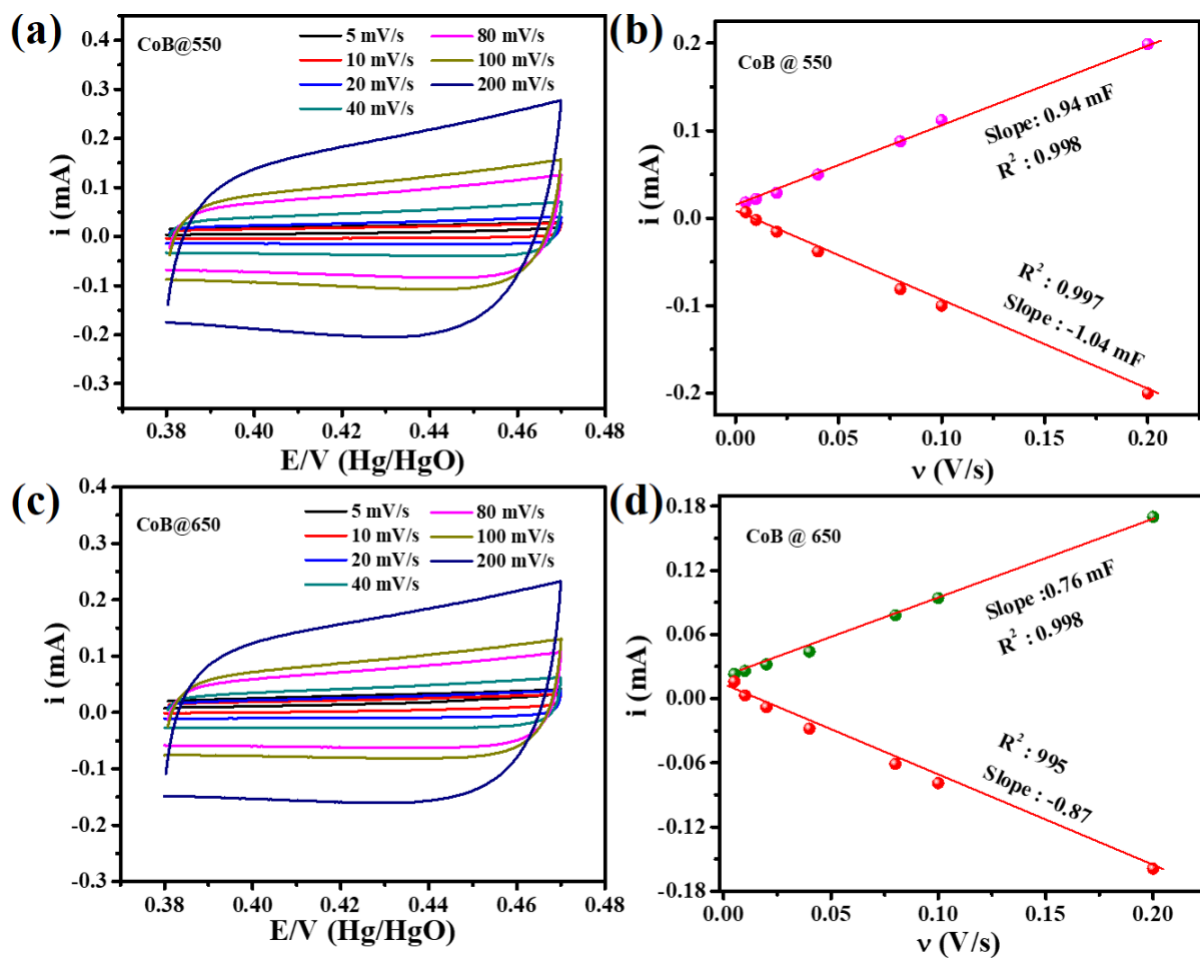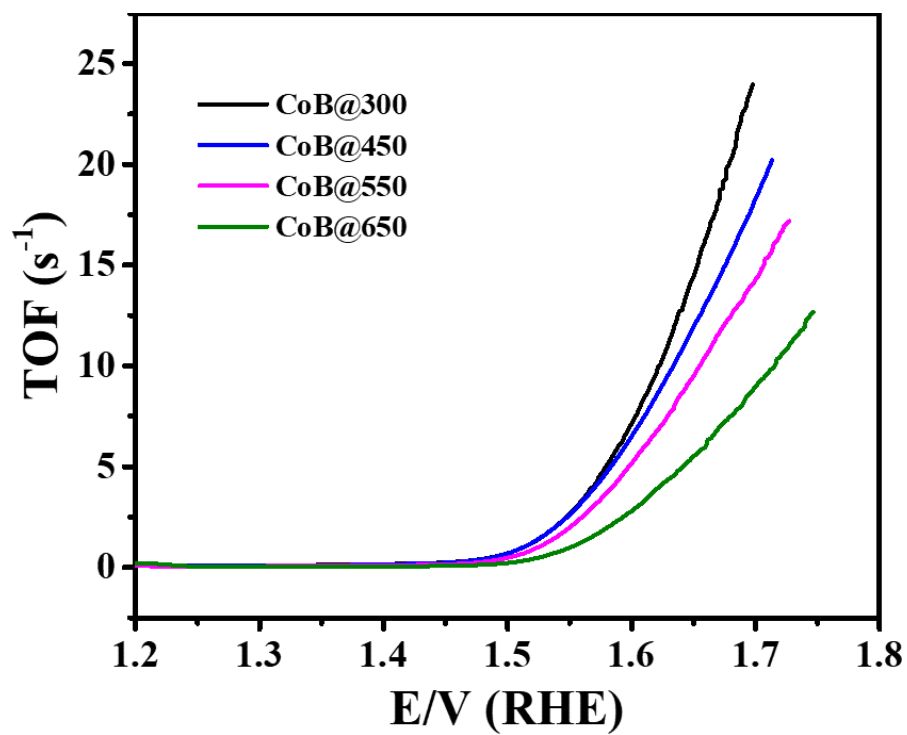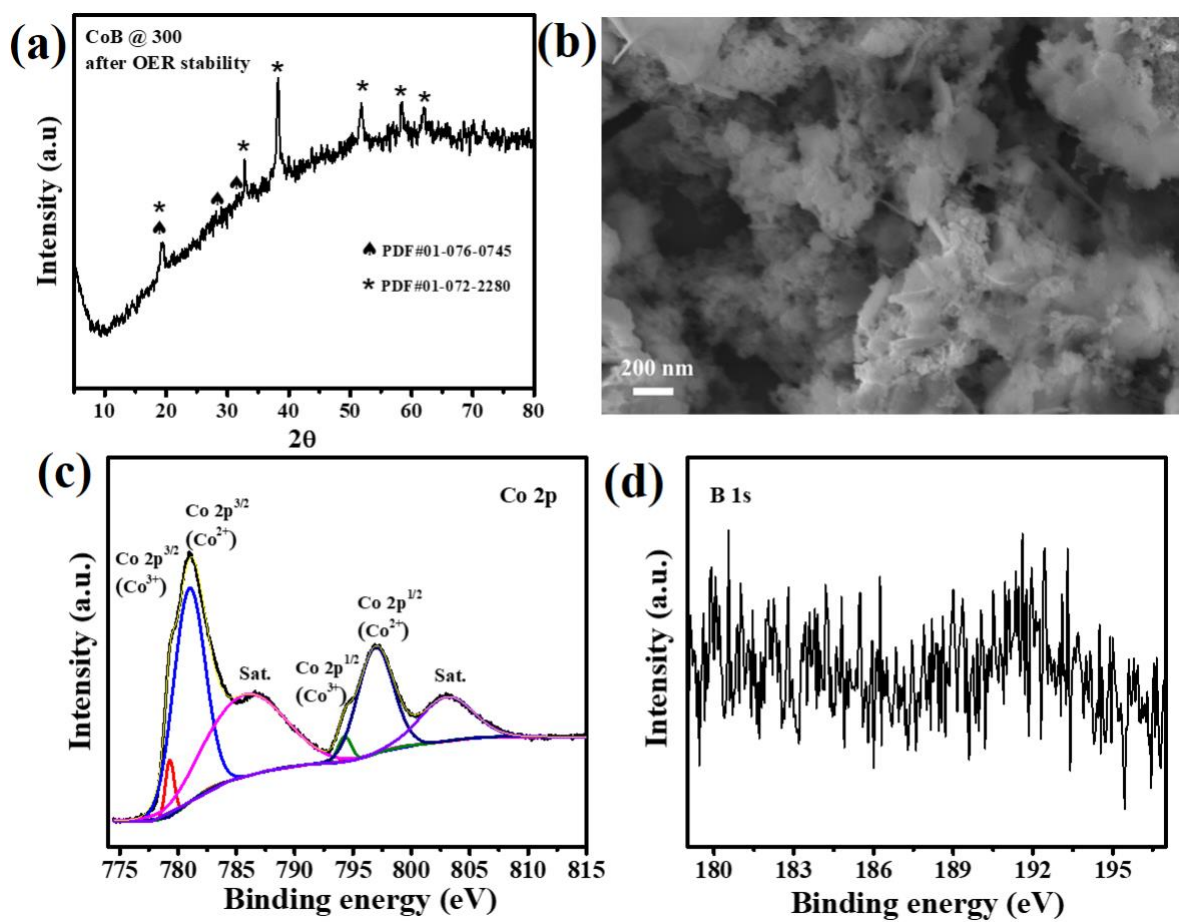
Fig. S 8 (a, c) Cyclic voltammograms and (b, d) plot of current at different sweep rate for CoB@550 and CoB@650.

Fig. S 9 Plot showing the turnover frequency for CoB@300, CoB@450, CoB@550 and CoB@650.

Fig. S 10 (a) X-ray diffraction pattern, (b) FESEM, high-resolution X-ray photoelectron spectrum for (c) Co 2p and (d) B 1s of CoB@300 after 15 hours of electrolysis.

Table S 2 Table showing the comparison of the electrocatalytic activity of CoB with the reported literatures.

Catalysts	Electrolyte (Conc.)	Overpotential (mV) @10 mA/cm^{-2}	Tafel Slope (mV/dec)	References
Ni-Co-B	1M KOH	300	113	[5]
Ni$_x$B-300	1M KOH	380	89	[6]
Ni-B @ Ni(OH)$_2$ @ Ni foam	1M KOH	300@ 100mA/cm^{-2}	49.0	[7]
Ni-Fe-B/rGO	1M KOH	265	58	[8]
Ni$_X$B/f-MWCNT	1M KOH	286	46.3	[9]
Co-B/C	1M KOH	320	75.00	[10]
Co-B/NF	1M KOH	315	56.00	[7,11]
Co-3Mo-B	1M NaOH	320	155.0	[12]
Fe$_2$B	1M KOH	296	52.4	[13]
Fe$_X$B	1M KOH	260	57.9	[14]
Ni-B$_i$@NB	1M KOH	302	52.0	[15]
Ni-B-O @ Ni$_3$B	1M KOH	264	127.0	[16]
NiB	1 M KOH	240	58	[17]
Ni$_3$B	1 M KOH	300	43	[18]
CNBO-NSs	1 M KOH	300	60	[19]
Co-Ni-B @NF	alkaline	313	120	[20]
CoFe-B	1M KOH	261	61	[21]
CoB@300	**1M KOH**	**290**	**62**	**Present work**

Table S 3 Table showing the OER activity of different catalysts.

Sample	η@10 mA/cm² (mV)	η@50 mA/cm² (mV)	Tafel slope (mV/dec.)	ECSA (cm²)	Roughness factor (R_f)	TOF (s⁻¹) @η=400 mV
Co@300	290	360	62	63.75	910.7	11.25
Co@450	295	375	76	55.10	787.1	9.78
Co@550	300	392	78	24.75	353.5	7.70
Co@650	355	441	82	20.37	291.0	4.39

References:

1   F. Herren, A. Ludi, P. Fischer and W. Halg, *Inorg. Chem.*, 1980, **19**, 956–959.

2   B. Bal, S. Ganguli and M. Bhattacharya, *J. Phys. Chem.*, 1984, **88**, 4575–4577.

3   R. K. Tripathy, A. K. Samantara and J. N. Behera, *Dalton Trans.*, 2019, **48**, 10557–10564.

4   L. Trotochaud, J. K. Ranney, K. N. Williams and S. W. Boettcher, *J. Am. Chem. Soc.*, 2012, **134**, 17253–17261.

5   S. Wang, P. He, Z. Xie, L. Jia, M. He, X. Zhang, F. Dong, H. Liu, Y. Zhang and C. Li, *Electrochim. Acta*, 2019, **296**, 644–652.

6   J. Masa, I. Sinev, H. Mistry, E. Ventosa, M. de la Mata, J. Arbiol, M. Muhler, B. Roldan Cuenya and W. Schuhmann, *Adv. Energy Mater.*, 2017, **7**, 1700381.

7   X. Liang, R. Dong, D. Li, X. Bu, F. Li, L. Shu, R. Wei and J. C. Ho, *Chem Cat Chem*, 2018, **10**, 4555–4561.

8   L. An, Y. Sun, Y. Zong, Q. Liu, J. Guo and X. Zhang, *J. Solid State Chem.*, 2018, **265**, 135–139.

9   X. Chen, Z. Yu, L. Wei, Z. Zhou, S. Zhai, J. Chen, Y. Wang, Q. Huang, H. E. Karahan, X. Liao and Y. Chen, *J. Mater. Chem. A*, 2019, **7**, 764–774.

10   Y. Li, H. Xu, H. Huang, L. Gao, Y. Zhao and T. Ma, *Electrochem. commun.*, 2018, **86**, 140–144.

11   Z. Chen, Q. Kang, G. Cao, N. Xu, H. Dai and P. Wang, *Int. J. Hydrogen Energy*, 2018, **43**, 6076–6087.

12   S. Gupta, N. Patel, R. Fernandes, S. Hanchate, A. Miotello and D. C. Kothari, *Electrochim. Acta*, 2017, **232**, 64–71.

13   H. Li, P. Wen, Q. Li, C. Dun, J. Xing, C. Lu, S. Adhikari, L. Jiang, D. L. Carroll and

S. M. Geyer, *Adv. Energy Mater.*, 2017, **7**, 1700513.

14   L. Wang, J. Li, X. Zhao, W. Hao, X. Ma, S. Li and Y. Guo, *Adv. Mater. Interfaces*, 2019, **6**, 1801690.

15   W. J. Jiang, S. Niu, T. Tang, Q. H. Zhang, X. Z. Liu, Y. Zhang, Y. Y. Chen, J. H. Li, L. Gu, L. J. Wan and J. S. Hu, *Angew. Chemie - Int. Ed.*, 2017, **56**, 6572–6577.

16   W. Yuan, X. Zhao, W. Hao, J. Li, L. Wang, X. Ma and Y. Guo, *Chem Electro Chem*, 2019, **6**, 764–770.

17   R. K. Tripathy, A. K. Samantara and J. N. Behera, *Sustain. Energy Fuels*, 2021, **5**, 1184–1193.

18   J. Li, H. Chen, Y. Liu, R. Gao and X. Zou, *J. Mater. Chem. A*, 2019, **7**, 5288–5294.

19   T. He, J. M. V. Nsanzimana, R. Qi, J. Y. Zhang, M. Miao, Y. Yan, K. Qi, H. Liu and B. Y. Xia, *J. Mater. Chem. A*, 2018, **6**, 23289–23294.

20   N. Xu, G. Cao, Z. Chen, Q. Kang, H. Dai and P. Wang, *J. Mater. Chem. A*, 2017, **5**, 12379–12384.

21   Y. X. Yang, B. L. Li, Q. Zhang, W. H. Guo, X. H. Wang, L. J. Li, H. Q. Luo and N. B. Li, *Energy Technol.*, 2021, **9**, 2000178.